

A LASER-INDUCED INCANDESCENCE SYSTEM FOR MEASURING SOOT FLUX IN AIRCRAFT ENGINE EXHAUSTS

T. P. Jenkins*, J. L. Bartholomew[†], and P. A. DeBarber[‡]
MetroLaser, Inc., Irvine, CA

P. Yang[§] and J. M. Seitzman**
Georgia Institute of Technology, Atlanta, GA

R. P. Howard^{††}
Sverdrup Technology, Inc., AEDC, TN

Corresponding author: tjenkins@metrolaserinc.com

AIAA/ASME/SAE/ASEE Joint Propulsion Conference, July 7 – 10, 2002, Indianapolis

Abstract

To address the need for measuring soot flux from aircraft engines, a system employing laser-induced incandescence (LII) has been developed for measuring soot concentration and velocity, with the potential for measuring particle size. The instrument instantaneously images up to a 1-m chord of an exhaust plume with a spatial resolution of 5.1 cm, and is capable of providing measurements of soot concentration down to $5 \mu\text{g}/\text{m}^3$. Quantitative non-intrusive measurements of soot concentration in the exhaust of a full-scale aircraft engine have been demonstrated using this system, and are presented here. The system enables rapid measurements, taking a data point every 0.1 seconds. Results are also presented from laboratory experiments with this system demonstrating velocity measurement and the potential for particle sizing. Measurements using this system should help to improve the monitoring of soot emissions from aircraft engines.

Introduction

The need is growing for accurate measurements of soot concentration in aircraft engine exhausts. New criteria on infrared plume signatures of military aircraft may render the current methods of measuring soot concentration unable to meet the necessary requirements of high temporal and spatial resolution. Air quality studies are continuing to underscore the importance of having accurate estimates of particulate emissions from all sources, including aircraft, due to adverse health effects that include premature death, aggravated asthma, and chronic bronchitis.¹

Conventional diagnostics tend to be intrusive and slow, requiring the extraction of gas samples. Advanced diagnostics are needed to improve emission inventories, and to aid in the development of cleaner burning engines. Here a new instrument is introduced employing laser-induced incandescence (LII) that shows promise as an improved method for quantifying soot flux from aircraft engines.

LII involves heating soot particles via laser radiation to the vaporization temperature, and measuring the resulting incandescence with a light-sensitive detector.² The resulting signals are sensitive to soot mass concentration and, to a lesser degree, to soot particle size. Quantitative soot concentration measurements of high accuracy can be elusive due to unwanted effects of particle size and shape.³ However, the errors can be minimized with the proper choice of detection wavelength, prompt gating, and high laser intensities.⁴ LII methods are becoming popular for measuring soot distributions in flames^{5,6} due to their potential for high spatial resolution. Recent efforts have been undertaken to apply LII to measurements in practical systems such as aircraft engine exhausts.^{7,8} However, the reported LII work in practical devices thus far has focused mostly on qualitative data.

Particle Vaporization Velocimetry (PVV)⁹ is a technique for non-intrusive velocity measurements in particle-laden flows. The method involves tagging the flow by vaporizing a region of soot particles, then imaging the region a short time later after it has been convected by the flow. PVV is ideally suited for velocity measurements in an aircraft engine exhaust since particles are naturally present and the measurement does not disturb the flow.

An LII-based system has been developed with the aim of being able to make quantitative measurements in an aircraft engine exhaust of soot mass concentration, velocity, and particle size. This system has enabled quantitative non-intrusive real-time measurements of soot concentration in a full-scale aircraft engine plume. These are, to our knowledge, the first quantitative LII

* Senior Scientist, AIAA member

[†] Scientist

[‡] Dir. Of Tech. Development, Senior Member

[§] PhD student, AIAA student member

** Assoc. Professor, AIAA Senior Member

^{††} Principle Investigator, AIAA Senior Member

Copyright © 2002 by MetroLaser, Inc.; Published by the American Institute of Aeronautics and Astronautics, Inc. with permission.

measurements in an aircraft plume. The system also shows promise for making measurements of velocity in an engine plume as well, and potentially particle size. This paper describes the design of the system, reports on laboratory experiments demonstrating system performance, and shows results from a full-scale engine test.

Experiment

Figure 1 shows a sketch of the LII system, mounted in an engine test cell. Two pulsed Nd:YAG lasers are used, each at a 10 Hz pulsing rate, one operating at 1064 nm and the other at 532 nm. Each pulse represents a measurement of soot concentration, thus a new measurement is obtained every 0.1 s. The 1064-nm beam is used for soot concentration measurements at low power, and to mark a region of the flow for velocimetry by vaporizing soot at high power. The 532-nm beam is formed into a sheet and is used for imaging the flowfield for velocimetry measurements, and potentially for scattering measurements for particle sizing. To avoid potential problems from the high level of engine noise, the lasers were housed in a separate room, adjacent to the test cell. The beams were directed through the wall into the test cell and across the plume into a beam dump. A camera captured LII emission from the measurement location in the plume at an angle 9° from direct backscatter. This geometry allowed a single vantage point from which both the beam-projecting optics and the detection optics could be mounted. The detection unit was mounted to a motorized stage that enabled translation in the vertical direction across the plume.

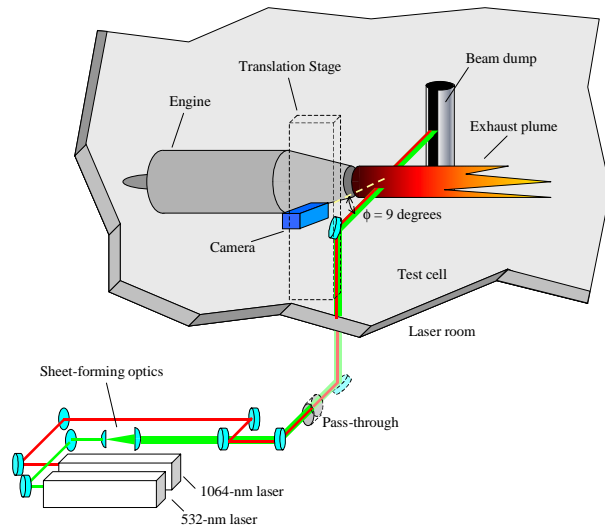


Figure 1. LII system for measuring soot concentration in aircraft engine exhausts.

The angled imaging geometry produces a distorted image that requires correction. Figure 2 shows the geometry. The condition whereby an object viewed at

an oblique angle is brought into focus by tilting the image plane is known as the Scheimpflug condition¹⁰, and the equations required for correcting the image are readily available.¹¹

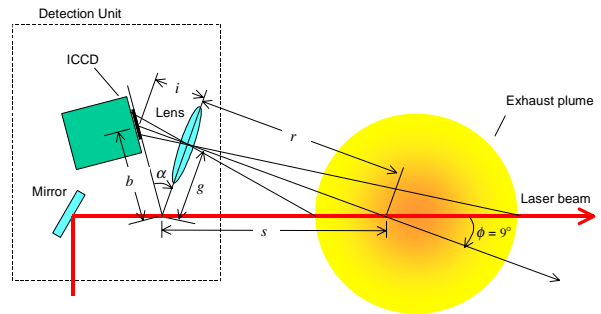


Figure 2. Geometry of the LII imaging system.

Figure 3 shows an uncorrected image taken with the system of a 1-inch x 1-inch grid placed in the object plane. A 3/4-inch long screw is standing on the plane of the grid to help orient the viewer. The distortion in Figure 3 is apparent in that the horizontal lines are not parallel and the spacing between the vertical lines decreases as one moves toward the left. The head of the screw is in focus since it is in the object plane, while the threads are out of focus. The entire grid is in focus since it is in the object plane, although the resolution decreases toward the far end of the grid. Figure 4 shows the image corrected by applying the equations in Reference 11, in which a new spatial coordinate has been assigned to each pixel. It can be seen that the parallelism of the horizontal lines and the even spacing between vertical lines have been restored.

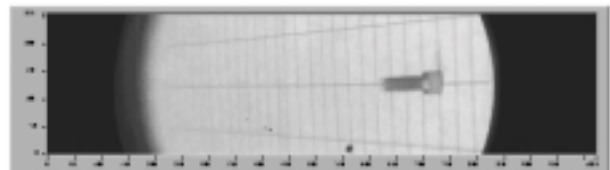


Figure 3. Uncorrected image of a 1" x 1" grid placed in the measurement plane of the LII system.

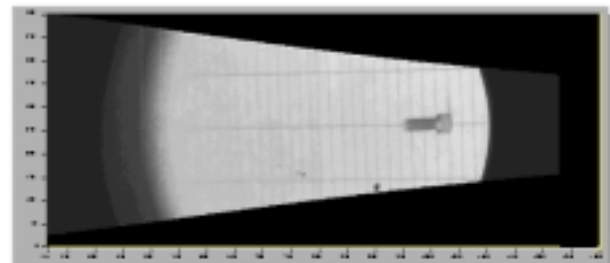


Figure 4. The same image in Figure 3 after correction.

The LII system was evaluated and calibrated in a laboratory. A device was developed for these purposes that produces a steady stream of simulated soot aerosol

at a known mass concentration. Figure 5 depicts this “soot generator”, which operates as follows. A solution of carbon black in water is placed in a humidifier that atomizes the liquid into small droplets. A continuous flow of air passes through the humidifier, bringing the droplets through a heated tube where they are dried, producing an aerosol of carbon particles suspended in air and water vapor. The aerosol exits from a straight tube 16 mm in diameter. The mass concentration of the aerosol can be calculated from the concentration of carbon in the solution, the air flow rate, and the loss rate of solution.

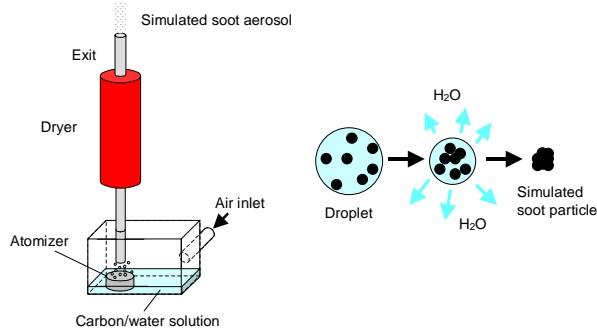


Figure 5. Soot generator to create an aerosol stream of carbon black particles that resemble soot.

Assuming that all of the carbon contained in a single droplet forms into a particle when the water evaporates, the diameter of the particles exiting the soot generator can be calculated. The atomizer was operated at a fixed condition so the droplet size distribution was constant, and was measured using a phase Doppler particle analyzer (PDPA), revealing that the mean droplet diameter was about 20 μm . Thus varying the carbon concentration in the solution varied particle size along with the aerosol concentration. For example, the particle diameter calculated that corresponds to an aerosol concentration of 1.2 mg/m^3 is 327 nm. Images taken with a scanning electron microscope of samples from the soot generator confirm that the particle sizes at this concentration were near this size.

Results

Concentration Validation Measurements

Figure 6 shows measured LII signals over four decades of aerosol concentration using an earlier version of the soot generator.³ The same LII techniques developed in Reference 3 were incorporated into the present system. The earlier data appear as open symbols, while data from the present LII system using the new soot generator described above appear as solid symbols. Note that the signal remains nearly linear with aerosol mass concentration over a large range of concentrations. Since the particle sizes change by a factor of 30 over this range of concentrations, it can be concluded that particle size effects are unimportant

using the techniques employed here, and that soot mass concentration is essentially proportional to the LII signal. Soot aerosol concentrations of 0.12 and 1.2 mg/m^3 were examined with the present system. It can be seen in Figure 6 that the resulting LII signals show linearity with aerosol mass concentration similar to the earlier data. These concentrations fall within the range of soot aerosol concentrations expected from engine tests, based on a previous study¹² using extractive sampling with a condensation nuclei counter and an electrostatic aerosol classifier. From Reference 12, the soot volume fractions are expected to range from 8×10^{-13} to 7×10^{-9} , corresponding to aerosol mass concentrations from 1.6×10^{-3} to $14 \text{ mg}/\text{m}^3$.

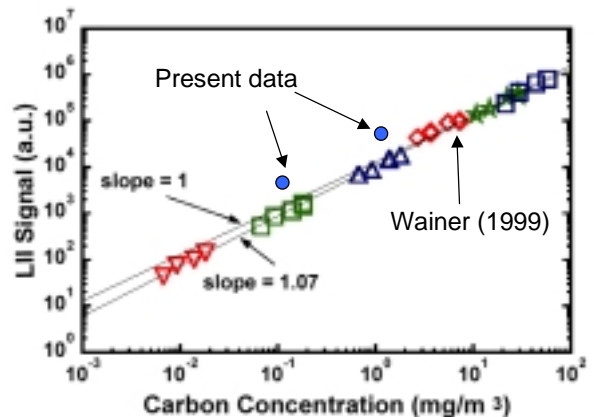


Figure 6. Comparison of present concentration data with data from earlier experiments.

Velocity Validation Measurements

For velocimetry measurements, the Nd:YAG laser operating at 1064 nm was used for marking the flow by vaporizing soot particles. The imaging pulse came from the second Nd:YAG laser operating at 532 nm. The 532-nm beam was formed into a sheet 40 mm wide by 7 mm thick, oriented with the width parallel to the flow direction. By setting the 1064-nm beam to a high energy, most of the soot particles in its path are vaporized, thus leaving a void of particles in the soot field. The flow convects this void downstream at the local flow velocity. An image is obtained using an ICCD camera during the subsequent pulse from the 532-nm laser sheet; thus, the velocity can be determined from the movement of the hole in a time of flight fashion.

Experiments were conducted in the laboratory to measure velocities in the soot generator flow. The soot generator was placed where the plume is in Figure 1, with the flow direction upward. Figure 7 shows two LII images formed by the 532-nm sheet passing through the flow field, in which a hole burned by the 1064 nm beam is visible. The image is cigar shaped, corresponding to the shape of the cross-section of the laser sheet in this near-backscatter configuration. In Figure 7, the laser

passes from right to left, and the flow moves from bottom to top. In Frame 1, the image was taken at essentially the same time as the marking pulse, while the image of Frame 2 was taken 5 ms later. The movement of the center of the hole was measured to be 5.6 ± 0.3 mm, corresponding to a velocity of 1.1 ± 0.1 m/s. The value is in good agreement with the average velocity computed from the measured airflow rate, which was 1.2 m/s.

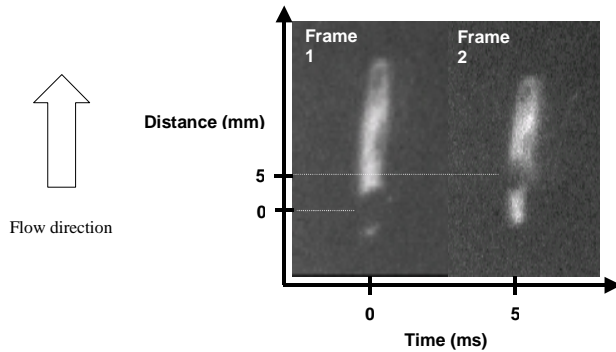


Figure 7. Instantaneous LII images demonstrating PVV for velocity measurements in the soot generator. A “hole” burned with the 1064-nm beam marks the flow for velocimetry.

In the engine plume, the velocities will be about two orders of magnitude greater, but the dimensions of the laser sheet will be the same. The resolution in the velocity measurement is limited by the accuracy with which the distance moved by the hole can be measured. Thus, the uncertainty in velocity should be about the same, or about 10 %. Potential improvements in accuracy may be obtained by using a CCD with a larger array. Using an array of 1000 x 1000 elements, which is readily available commercially, should reduce the uncertainty in velocity to about 1%.

Particle Sizing Validation Measurements

The same two lasers that were used for velocimetry were also used for measurements to investigate the potential of particle sizing using the scattering/LII ratio method. This method relies on the fact that scattered light changes in a different way with particle size than incandescent light. A model¹³ has been developed based on Mie theory for scattering from a cloud of soot particles with the optical properties and size distribution of those expected in a jet engine exhaust. The model shows that an unambiguous scattering signal exists for particles smaller than 65 nm.¹³ Particles in the exhaust are expected to have sizes in the range 20 – 40 nm¹², so this method should apply. Since the LII signal depends on mass concentration only, and not appreciably on particle size, the scattered light signal normalized by the LII signal provides a sensitive measure of particle size.

Scattering measurements were obtained in the soot generator to test this method. Images of scattered light were collected during pulses from the 532-nm laser at 9° from backscatter with an unfiltered camera. LII images were collected for the same conditions from the 1064-nm laser. Table 1 shows the resulting signals in arbitrary units for the two concentrations examined, 0.12 and 1.2 mg/m³. These concentrations correspond to particle sizes of 152 nm and 327 nm, respectively. The last column of the table gives the ratio of the scattering signal to the LII signal. It can be seen that as the particle size increases from 152 nm to 327 nm, the ratio of scattering/LII decreases from 29.9 to 18.0. Although the particle sizes are larger in this test than in the expected size range for exhaust measurements, this reduction in the scattering/LII ratio for this change in particle size is consistent with the model predictions. For smaller particles, the ratio will monotonically increase with size for diameters up to 65 nm.¹³ These results suggests that the scattering/LII ratio technique will be useful for obtaining estimates of particle sizes in a jet engine exhaust.

Table 1. Measured signals for testing the particle sizing technique.

Soot Concentration (mg/m ³)	Estimated particle diameter (nm)	Measured LII signal (binned counts)	Measured scattering signal (binned counts)	Ratio Scatt/LII
.12	152	3.75×10^3	1.12×10^5	29.9
1.2	327	6.76×10^4	1.22×10^6	18.0

Figure 8 shows an example of a raw image of LII in the exhaust plume during an engine test, uncorrected for distortion. The LII appears as a thick line where the laser beam intersects the plume as seen by the camera in this near-backscatter arrangement. In this image, the exhaust flow is from left to right, and the laser beam propagation direction is from bottom to top. This image is an accumulation of 20 exposures from 20 pulses obtained over a period of 2 seconds. Spatial variations in intensity due to variations in soot concentration along the beam path can be seen. The spatial resolution, limited by the LII path length as discussed above, is 5.1 cm. Because the angle between the viewing axis and the laser beam path, nominally 9 degrees, varies from one side of the LII image to the other, the path length through the soot that is imaged onto the camera will vary from pixel to pixel, changing by about 20 percent from one end of the illuminated section of the beam to the other. Consequently, to obtain quantitative soot concentrations from the image, the measured intensity was multiplied by a correction factor equal to the ratio of the calibration path length to the actual path length. This correction factor is easily calculated from knowledge of the system geometry.

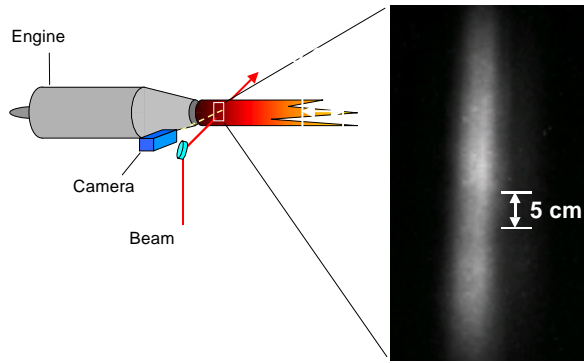


Figure 8. Image of LII from soot in an aircraft engine exhaust plume.

Data were obtained during engine tests over a period of about six hours. These images were processed to obtain quantitative soot concentrations by summing pixels across the beam. Due to the distortion, a greater number of illuminated pixels would be summed on the side closest to the camera than on the far side. This effect was accounted for by applying the appropriate correction factor to each summed row of pixels, obtained from knowledge of the collection system geometry. Data rates were dependent on the laser pulsing rate, with a data point obtained every 0.1 seconds. For long durations of data collection, accumulations of ten images were stored, corresponding to 1 second between data points, for a total of 3000 seconds, long enough to cover an entire mission.

Calibration images were obtained by placing the soot generator at the measurement location and capturing images while the engine was not running. However, it should be noted that a flow meter problem limited the accuracy of the calibration for the measurements reported herein. It is estimated that the uncertainty in the stated soot mass concentrations is on the order of 300 percent, but this was not quantified by measurement. This large uncertainty is not inherent to the technique. With a properly functioning flow meter the uncertainty in the measurements would be dominated by the uncertainty in the characteristic particle size. This translates to a systematic uncertainty in the LII signal of about 40 percent if no information about particle size is known, and lower with some knowledge of particle size. In any case, spatial and temporal relations among the present data will be accurate.

The engine tests during collection of these data were designed to simulate an actual mission, so a variety of power setting changes occurred throughout each engine test. Figure 9 shows a sequence of data from about 20 binned images, in which soot mass concentration is plotted as a function of the transverse coordinate across the plume, s , and time, t . Each transverse profile

represents one second of data, for a total of about 20 seconds in the figure. It can be noted that details of instantaneous soot distributions in the plume are revealed. An examination of the noise level indicates that concentrations down to $5 \mu\text{g}/\text{m}^3$ can be detected. During this series of measurements, the throttle setting, indicated along the left side of Figure 9, was rapidly adjusted from the high cruise to the intermediate power settings. Figure 9 reveals that immediately after the throttle increase, the soot concentration jumps up to about $1.5 \text{ mg}/\text{m}^3$, remains there for a few seconds, and then falls sharply to a steady value of about $0.3 \text{ mg}/\text{m}^3$. These trends observed in going from a lower to a higher power setting were consistent throughout the data. Figure 10 shows an example in which two kinds of power transitions can be observed: first low-to-high, then a few seconds later high-to-low. During the high-to-low transition a momentary decrease in soot concentration can be seen.

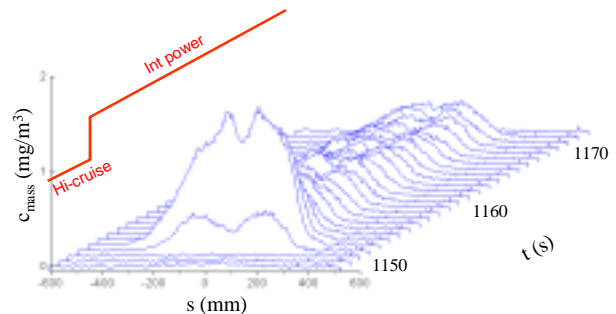


Figure 9 Soot mass profiles in an engine exhaust for a transition from high cruise to intermediate power.

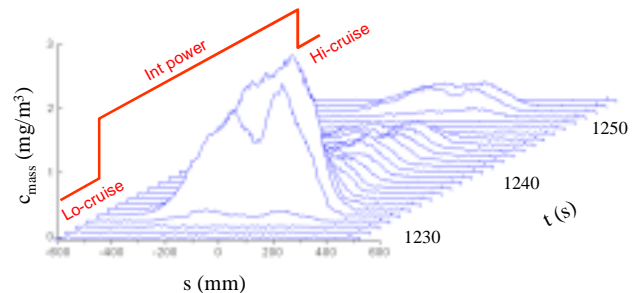


Figure 10. Transverse profiles of soot concentration showing both low-to-high and high-to-low power changes.

By integrating the soot concentration profiles along the transverse coordinate, s , and dividing by the characteristic plume diameter, 0.5 m, an average soot concentration across the plume was obtained. Figure 11 shows the integrated averages for a portion of an entire mission plotted as a function of time. During this experimental run the data were continuously collected and stored throughout a 46-minute mission. The optics stayed aligned throughout this run, as was checked by noting that the position of the beam was the same on raw images taken before and after the run. The power

settings for the mission appear at the top of the plot. In Figure 11 it can be seen that each low-to-high power transition is accompanied by a large momentary surge in soot concentration

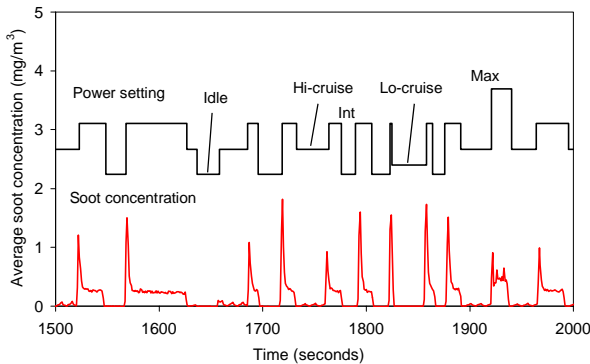


Figure 11. Soot mass concentration averaged across the plume during a mission.

Discussion

In a typical application of LII, the detection optics are aligned at a right angle to the direction of the laser beam propagation. This arrangement produces the shortest path length through the beam, and hence the best spatial resolution. However, detection at right angles requires access to the measurement location from two sides. In an engine test cell environment, components of the measurement system must be able to stand up to severe vibration as well as aerodynamic forces. There are few locations within a typical test cell that are suitable for optical components to be mounted to during engine tests. Thus, a measurement system that requires access from only one side has a distinct advantage, since it requires only one mounting location. By incorporating an oblique imaging geometry, this design has a single vantage point and enables spatially resolved LII measurements across an entire plume cross-section.

A significant amount of information can be obtained from transverse profiles like those of Figure 9 and Figure 10. This data is collected in real time, and is available immediately after the measurements. The spatial distributions of soot may help engine designers to evaluate the effects of engine design changes, such as to augment components. For example, the bimodal and asymmetric character of the soot concentration profiles may provide valuable information on mixing in the exhaust stream. In the present results consistent trends were observed that could have relevance to design issues; a surge of soot occurred in all cases of transitioning to higher power, and a local minimum in soot concentration appears in the middle of the plume during each surge. Because the presence of soot indicates inefficient combustion, the monitoring of

surges in soot concentration during operation may help engine designers to optimize for efficiency.

Information gained from tests such as those shown in Figure 11 may perhaps help mission planners to evaluate the consequences of certain maneuvers to plume signature; some maneuvers might be observed to produce more soot, and hence higher IR signature, than others.

The velocity and particle sizing methods examined here appear to be ideally suited for measurements in an aircraft engine exhaust. These methods are awaiting testing in the engine test cell environment. As outlined above, the results from laboratory testing are encouraging for both of these methods.

Conclusions

An LII system for measuring soot concentrations in turbine engine exhausts has been developed, installed in an engine test cell, and successfully demonstrated. Additional capabilities of velocimetry and particle sizing have also been developed and tested in a laboratory, and show promise for use in actual aircraft engine tests. Spatially resolved, real-time, non-intrusive soot concentration measurements were made in the exhaust of an aircraft engine during ground testing that compliment the capabilities of current measurement techniques. The system enables rapid data collection, with a measurement every 0.1 seconds. The rugged design enabled the system to operate well throughout a six-hour period of continuous engine testing, despite the harsh environment of the test cell. Initial tests showed that large variations in the overall soot mass concentration correlated with changes in engine power settings, especially when going from a lower to a higher power setting. Data such as these should be valuable to military mission planners in reducing IR signatures as well as to engine designers for monitoring engine operation.

ACKNOWLEDGMENTS

This effort was sponsored by a contract under the Arnold Engineering Development Center, Air Force Materiel Command, USAF.

REFERENCES

- ¹ United States Environmental Protection Agency, Office of Air & Radiation, Office of Air Quality Planning & Standards, "Health and Environmental Effects of Particulate Matter", website: <http://www.epa.gov/ttn/oarpg/naaqsfm/pmhealth.html>, (2002)
- ² Melton, L. A., "Soot Diagnostics Based on Laser Heating", *Appl. Optics* **23**, 2201 (1984).

-
- ³ Wainner, R. T., "An Analytic and Quantitative Analysis of the Laser-Induced Incandescence of Soot", PhD Thesis, Georgia Institute of Technology, (1999).
- ⁴ Mewes, B. and Seitzman, J. M., "Soot Volume Fraction and Particle Size Measurements with Laser-Induced Incandescence", *Applied Optics* **36**, pp. 709-717 (1997).
- ⁵ Shaddix, C. R. and Smyth, K. C., "Laser-Induced Incandescence Measurements of Soot Production in Steady and Flickering Methane, Propane, and Ethylene Diffusion Flames", *Comb. & Flame* **107**, 418 (1996).
- ⁶ Appel, J., Jungfleisch, B., Marquardt, M., Suntz, R. and Bockhorn, H., "Assessment of Soot Volume Fractions from Laser-Induced Incandescence by Comparison with Extinction Measurements in Laminar, Premixed, Flat Flames", *Twenty-Sixth Symp. (Int'l) on Comb.*, 2387, (1996).
- ⁷ Allen, M. G., Upschulte, B. L., Sonnenfroh, D. M., Rawlins, W. T., et al., "Infrared Characterization of Particulate Emissions from Gas Turbine Combustors", AIAA 2001-0789 (2001).
- ⁸ Schfer, K., Heland, J., Lister, D. H., et al., "Nonintrusive Optical Measurements of Aircraft Engine Exhaust Emissions and Comparison with Standard Intrusive Techniques", *Appl. Optics* **39**, 441 (2000).
- ⁹ Yang, P., Seitzman, J. M., and Wainner, R., "Particle vaporization velocimetry for soot-containing flows," AIAA 2000-0645 (2000).
- ¹⁰ A. K. Prasad and K. Jensen, Scheimpflug Stereocamera for Particle Image Velocimetry in Liquid Flows", *Applied Optics* **34**, pp. 7092-7099, 1995.
- ¹¹ S. Clausen and P. Astrup, "Oblique Laser-Sheet Visualization", *Applied Optics* **34**(19), pp. 3800-3805, 1995.
- 12 Howard, R. P., Hiers, R. S., Whitefield, P. D., Hagen, D. E., et al., "Experimental Characterization of Gas Turbine Emissions at Simulated Flight Altitude Conditions", AEDC-TR-96-3, (1996).
- 13 Jenkins, T. P., Bartholomew, J. L., and DeBarber, P. A., "A Real-Time Non-Intrusive Measurement System for Soot Properties in Aircraft Engine Exhausts", Final Report, USAF contract F40600-98-C-0014 (2002).